CWP-383
May 2001

Error in shear wave polarization and time splitting

Gwénola Michaud and Roel Snieder

This paper appeared in the May 2001 CWP Project Review, CWP-384.

Center for Wave Phenomena
Colorado School of Mines
Golden, Colorado 80401
303/273-3557

Error in shear wave polarization and time splitting

Gwénola Michaud* and Roel Snieder†
*Reservoir Characterization Project, Dept. of Geophysics, Colorado School of Mines
†Center of Wave Phenomena, Dept. of Geophysics, Colorado School of Mines

ABSTRACT
Any measurement of parameters contains uncertainties from data acquisition and processing. It is critical to evaluate these uncertainties not only to substantiate the interpretation of the measurements, but also to optimize the acquisition pattern for accurate measurements of the parameters of interest.

The objective of this analysis is to understand the uncertainty in the estimation of anisotropy parameters from shear waves recorded in a borehole seismic dataset. Shear wave polarization and time delay are studied as a function of acquisition uncertainties such as receiver and source misorientation, miscoupling, and band-limited random noise.

Key words: error propagation, shear wave polarization and splitting, noise estimation

Introduction

Measuring any parameter in geophysics involves data acquisition and processing. Since any data acquisition is neither exact and/or exactly reproducible, we have to estimate the errors or uncertainties in the data and ensure that they are as small as possible. Indeed, besides the signal we are interested in, recorded data contain "noise", an ambiguous term for defining the data, which cannot, or are chosen not to be explained (Scales, 1998). Therefore, understanding the uncertainty in the data and measurements is critical to justify the data interpretation.

Few studies have focused on the error associated with the estimation of anisotropy parameters due to noise and acquisition uncertainties. Knowlton (1996) presented uncertainties in three component receiver orientation in borehole data from time picking on compressional waves. Li (1993) analyzed changes in shear wave time splittings for different signal to noise ratios and methodologies. However, shear wave time splitting for instance in Vacuum Field, New Mexico is about 10 ms for surface seismic reflections for a reservoir interval of 600 ft. Since errors due to acquisition and noise contamination can exceed few ms, a comparison in time delay between different surveys may not be statistically significant. It is critical to address and estimate the uncertainty of measurement to justify the use of seismic attributes such as shear wave polarization angle and time delay for time-lapse analysis, for instance. This paper presents the error analysis in estimating shear wave polarization and time delay as a function of systematic errors in the acquisition and random noise.

Shear Wave Polarization Angle and Time Delay

Four component (4-C) shear wave data, recorded with two horizontal sources and receivers, are expressed as:

$$\tilde{\mathbf{D}}(\mathbf{t}) = \begin{bmatrix} D_{11}(t) & D_{12}(t) \\ D_{21}(t) & D_{22}(t) \end{bmatrix},$$

where, $D_{ij}(t)$ is the recorded data at the receiver component, i, from the source component, j. Considering the Earth as a linear system for the propagation of the seismic waves, the recorded traces satisfy the convolution model (Zeng, 1993):

$$\tilde{\mathbf{D}}(\mathbf{t}) = \tilde{\mathbf{G}}(\mathbf{t}) * \tilde{\mathbf{M}}(\mathbf{t}) * \tilde{\mathbf{S}}(\mathbf{t}) \quad (1)$$

with the geophone response, $\tilde{\mathbf{G}}(\mathbf{t})$, the source signature, $\tilde{\mathbf{S}}(\mathbf{t})$, and the medium response for shear waves, $\tilde{\mathbf{M}}(\mathbf{t})$. The geophone and source responses, $\tilde{\mathbf{G}}(\mathbf{t})$ and $\tilde{\mathbf{S}}(\mathbf{t})$, are diagonal matrices with the principal components given

by the scalar functions of the in-line and crossline geophones and sources. The operation denoted by the asterisk (*) is a convolution in the time domain. The medium response matrix, $\tilde{\mathbf{M}}(\mathbf{t})$, expressed as:

$$\tilde{\mathbf{M}}(\mathbf{t}) = \tilde{\mathbf{R}}^{\mathbf{T}}(\theta)\tilde{\mathbf{\Lambda}}(\mathbf{t})\tilde{\mathbf{R}}(\theta). \quad (2)$$

represents the directional response of the medium. This medium response is seen as the combination of the geophone and source rotation matrices, $\tilde{\mathbf{R}}^{\mathbf{T}}(\theta)$ and $\tilde{\mathbf{R}}(\theta)$, with the matrix representing the propagation of the two shear waves, $\tilde{\mathbf{\Lambda}}(\mathbf{t})$. The fast shear wave polarization angle, θ, is relative to the inline direction given by the source and receiver locations. As demonstrated by (Alford, 1986), the simultaneous rotation of source and receiver enables us to retrieve the fast and slow shear wave particle motions along two orthogonal components, represented by the diagonal matrix, $\tilde{\mathbf{\Lambda}}(\mathbf{t})$:

$$\tilde{\mathbf{\Lambda}}(\mathbf{t}) = \begin{bmatrix} \lambda_1(t) & 0 \\ 0 & \lambda_2(t) \end{bmatrix}$$

where, $G_i(t) * \lambda_i(t) * S_i(t) = w(t-\tau_i)$ represents the wavelet recorded at the geophone component, $G_i(t)$, and generated from the shear source component, $S_i(t)$. The traveltime of the shear wave energy is denoted as τ_i. The wavelet, $w(t-\tau_i)$, is also represented as a function of the attenuation of each shear wave component: $w(t-\tau_i) = G_i(t) * a_i(t) * S_i(t-\tau_i)$, where, $a_i(t)$, the attenuation of the fast (i=1) and slow (i=2) shear waves (MacBeth, 1994). The previous definitions are based on perfect alignment and coupling of the sources and geophones.

During the data acquisition, sources and geophones can be misaligned, inducing errors in the results of the Alford rotation. Indeed, the source and receiver coordinate systems are then not rotated to the same angle. For a source misorientation relative to the inline direction, ϵ_S, the recorded data are expressed as (MacBeth, 1994):

$$\tilde{\mathbf{D}}(\mathbf{t}) = \tilde{\mathbf{G}}(\mathbf{t}) * \tilde{\mathbf{R}}^{\mathbf{T}}(\theta)\, \tilde{\mathbf{\Lambda}}(\mathbf{t})\, \tilde{\mathbf{R}}(\theta + \epsilon_{\mathbf{S}}) * \tilde{\mathbf{S}}(\mathbf{t}).$$

Similarly, for a receiver misorientation, ϵ_G, the recorded data are:

$$\tilde{\mathbf{D}}(\mathbf{t}) = \tilde{\mathbf{G}}(\mathbf{t}) * \tilde{\mathbf{R}}^{\mathbf{T}}(\theta - \epsilon_{\mathbf{G}})\, \tilde{\mathbf{\Lambda}}(\mathbf{t})\, \tilde{\mathbf{R}}(\theta) * \tilde{\mathbf{S}}(\mathbf{t}).$$

Source and receiver miscouplings infer relative differences in the amplitudes on the source or receiver components. As the shear wave polarization angle is estimated from the comparison of the diagonal and off-diagonal energy, the amplitude differences that are generated from miscoupling induce an error in shear wave polarization angle. The miscoupling of the source and receiver is defined according to a multiplicative coefficient, K_S and K_G, respectively. Recorded data presenting a source miscoupling are expressed as:

$$\tilde{\mathbf{D}}(\mathbf{t}) = \begin{bmatrix} D_{11}(t) & K_S D_{12}(t) \\ D_{21}(t) & K_S D_{22}(t) \end{bmatrix}.$$

Similarly, data recorded with a receiver miscoupling are:

$$\tilde{\mathbf{D}}(\mathbf{t}) = \begin{bmatrix} D_{11}(t) & D_{12}(t) \\ K_G D_{21}(t) & K_G D_{22}(t) \end{bmatrix}.$$

The source and receiver imbalance coefficients, K_S and K_G, may be frequency dependent (MacBeth, 1994). However, in the case considered here, these coefficients are considered as simple multiplicative constants.

Apart from misorientation and miscoupling issues, the recorded random noise is an additional uncertainty in the measurements. The recorded random noise is band-limited, and refers no longer to white noise, but "colored" noise. This leads to correlation in the different time samples of the noise within a record.

The sources of uncertainties are now defined. Their corresponding error in the estimation of shear wave polarization angle and time delay can be determined.

Shear Wave Polarization

The rotated data can be expressed as a function of the source and geophone misorientations (ϵ_S and ϵ_G) and miscouplings (K_S and K_G), from equations (1) and (2):

$$\tilde{\mathbf{G}}(\mathbf{t}) * \tilde{\mathbf{\Lambda}}(\mathbf{t}) * \tilde{\mathbf{S}}(\mathbf{t}) = \tilde{\mathbf{R}}(\theta_{\mathbf{G}})\, \tilde{\mathbf{D}}(\mathbf{t})\, \tilde{\mathbf{R}}^{\mathbf{T}}(\theta_{\mathbf{S}}), \quad (3)$$

where the angle of rotation for the receiver is $\theta_G = \theta - \epsilon_G$, and for the receiver, $\theta_S = \theta + \epsilon_S$, considering the source and receiver misorientation, ϵ_S and ϵ_G. Expanding equation (3), the rotated data are related to the source and receiver miscouplings:

$$\begin{aligned} &G_1(t) * \Lambda_{11}(t) * S_1(t) = \\ &\cos\theta_G \,(\, D_{11}(t)\cos\theta_S + \tfrac{1}{K_S} D_{12}(t)\sin\theta_S) + \\ &\frac{1}{K_G}\sin\theta_G \,(\, D_{21}(t)\cos\theta_S + \tfrac{1}{K_S} D_{22}(t)\sin\theta_S), \end{aligned}$$

$$\begin{aligned} &G_1(t) * \Lambda_{12}(t) * S_2(t) = \\ &\cos\theta_G \,(\, -D_{11}(t)\sin\theta_S + \tfrac{1}{K_S} D_{12}(t)\cos\theta_S) + \\ &\frac{1}{K_G}\sin\theta_G \,(\, -D_{21}(t)\sin\theta_S + \tfrac{1}{K_S} D_{22}(t)\cos\theta_S), \end{aligned}$$

$$\begin{aligned} &G_2(t) * \Lambda_{21}(t) * S_1(t) = \\ &\sin\theta_G \,(\, -D_{11}(t)\cos\theta_S - \tfrac{1}{K_S} D_{12}(t)\sin\theta_S) + \\ &\frac{1}{K_G}\cos\theta_G \,(\, D_{21}(t)\cos\theta_S + \tfrac{1}{K_S} D_{22}(t)\sin\theta_S), \end{aligned}$$

$$G_2(t) * \Lambda_{22}(t) * S_2(t) =$$
$$\sin\theta_G \left(D_{11}(t)\sin\theta_S - \tfrac{1}{K_S} D_{12}(t)\cos\theta_S \right) +$$
$$\frac{1}{K_G}\cos\theta_G \left(-D_{21}(t)\sin\theta_S + \tfrac{1}{K_S} D_{22}(t)\cos\theta_S \right).$$

The fast shear wave polarization angle corresponds to the angle, θ, that minimizes the energy of the off-diagonal components ($G_1(t) * \Lambda_{12}(t) * S_2(t)$ and $G_2(t) * \Lambda_{21}(t) * S_1(t)$) within the time window around the first break. This polarization angle is evaluated as a function of the miscoupling coefficient, the misalignment of the source and the receiver, and the band-limited random noise, $\tilde{\mathbf{N}}(\mathbf{t})$, added to the data, $\tilde{\mathbf{D}}(\mathbf{t})$:

$$\theta = \frac{1}{2}\left(\epsilon_G - \epsilon_S + \arctan \frac{\int \{K_G\, DN_{12}(t) + K_S\, DN_{21}(t)\}\, dt}{\int \{\, DN_{22}(t) - K_S\, K_G\, DN_{11}(t)\}\, dt} \right)$$

where $\tilde{\mathbf{DN}}(\mathbf{t}) = \tilde{\mathbf{D}}(\mathbf{t}) + \tilde{\mathbf{N}}(\mathbf{t})$.

The error in the polarization angle is now estimated according to the covariance and mean of the each parameter described previously, following the relation:

$$\sigma_\theta^2 = \left(\frac{\partial\theta}{\partial\epsilon_S}\right)^2 \sigma_{\epsilon_S}^2 + \left(\frac{\partial\theta}{\partial\epsilon_G}\right)^2 \sigma_{\epsilon_G}^2 + \left(\frac{\partial\theta}{\partial K_G}\right)^2 \sigma_{K_G}^2 + \left(\frac{\partial\theta}{\partial K_S}\right)^2 \sigma_{K_S}^2 + \sum_{ij} \left(\frac{\partial\theta}{\partial N_{ij}}\right)^2 \int\int C_{ij}(t,t')\, dt\, dt'. \quad (4)$$

The source and receiver misalignment and coupling are assumed uncorrelated. The uncertainty due to band-limited noise series is denoted $C_{ij}(t,t')$. Since the derivatives of the angle, θ, according to the noise samples are time invariant, the uncertainties, $C_{ij}(t,t')$, in the time samples of each noise record, N_{ij}, are integrated over the values of t and t' within the employed time windows. For simplicity, the correlation between different noise sampled are ignored.

The objective is to understand by means of a numerical example the influence of source and receiver coupling, misalignment and noise content on the estimation of the shear source polarization. The noise uncertainty is estimated as the covariance of the noise record. The fast and slow shear wave first breaks, over which the polarization angle is evaluated, are modeled in the synthetic example as one cycle of a sine function with a frequency of 30 Hz and a sampling rate of 2 ms. The data, $\tilde{\mathbf{D}}(\mathbf{t})$, are modeled with eq.(2) with the fast shear wave polarization angle oriented 30° regarding the source-receiver direction. The shear wave time splitting is set at 10 ms. The traces are contaminated with a Gaussian noise filtered with a band-pass filter of 10-20-70-90 Hz. In addition, the values of the noise are amplified to create different signal to noise ratios (S/N).

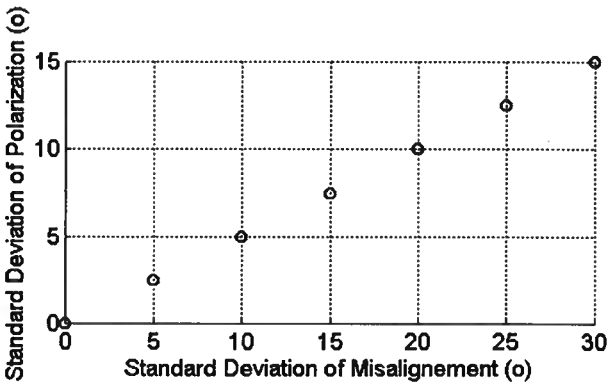

Figure 1. Standard deviation of shear wave polarization angle as a function of the standard deviation of receiver misalignment. The polarization angle error is half the angle of misorientation of the receiver.

The receiver misalignment is a major cause of uncertainty in shear wave polarization. Indeed, from eq.(5), the two first terms equal $(\frac{1}{2}\sigma_{\epsilon_i})^2|_{i=S,G}$. For an error in the receiver alignment only, the uncertainty in shear wave polarization angle is half the receiver misorientation angle (Figure 1). In addition, the band-limited noise induces an error even if the receiver and source are perfectly aligned and coupled. As presented in Figure 2, the error in polarization increases with a decreasing signal to noise (S/N) ratio. The error is less than 1°, for S/N more than 9 and about 5° for a S/N of 4. However, the error is larger than 15° for a S/N less than 2.

The receiver miscoupling is another source of error in the shear wave polarization. The error plotted as a function of the miscoupling coefficient, K_G, from 0.5 to 1.5, presents an expected increase of the error with the receiver miscoupling (Figure 3). The error in shear wave polarization angle increases up to 10° for a miscoupling of ±50% and no error in the receiver orientation, ϵ_G. Surprisingly, for an error of 50% in the miscoupling the standard deviation of polarization angle varies only by 3°, for a misalignment of 30°.

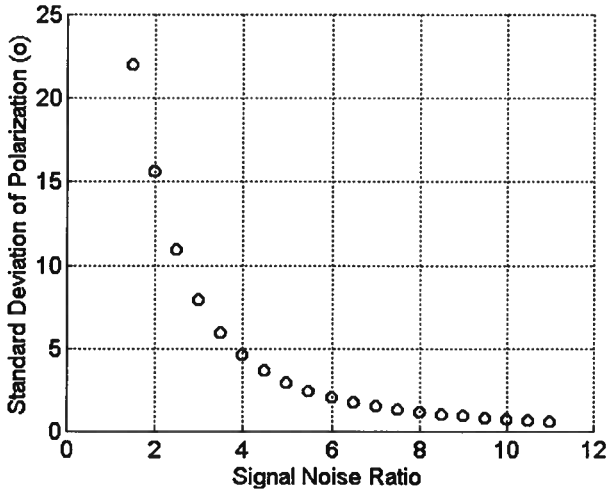

Figure 2. Standard deviation of shear wave polarization angle as a function of the signal to noise ratio. The polarization angle error is increasing with decreasing S/N ratio to attain up to 15° of error for a S/N less than 2.

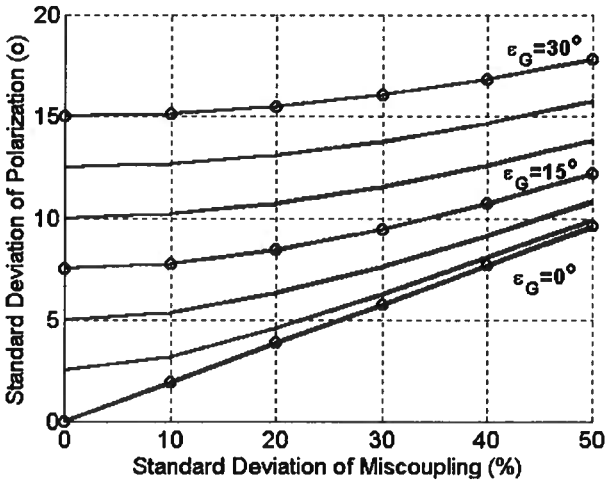

Figure 3. Standard deviation of shear wave polarization angle as a function of the receiver miscoupling (K_G) on the horizontal axis and misalignment (ϵ_G). For no receiver misalignment ($\epsilon_G = 0^o$), the uncertainty in shear wave polarization angle due to miscoupling is as large as 10^o, and only 3^o, for a misalignment (ϵ_G) of 30^o.

Shear Wave Time Splitting

Once the polarization angle is estimated, the fast and slow shear waves correspond with the two principal time series, $\lambda_1(t) = G_1(t) * \Lambda_{11}(t) * S_1(t)$ and $\lambda_2(t) = G_2(t) * \Lambda_{22}(t) * S_2(t)$. The shear wave time splitting is estimated by the maximum value of the cross-correlation, $\rho_{\lambda_1\lambda_2}(t)$. The cross-correlation function of the shear wave time series is given by:

$$\rho_{\lambda_1\lambda_2}(t) = \frac{\sigma_{\lambda_1\lambda_2}(t)}{\sqrt{\sigma_{\lambda_1}(0)\sigma_{\lambda_2}(0)}}.$$

$\sigma_{\lambda_1\lambda_2}(t)$ is the cross-covariance function, given by:

$$\sigma_{\lambda_1\lambda_2}(t) = \frac{1}{T}\int \lambda_1(s)\lambda_2(s+t)ds,$$

where, T is the window length around the first break. The covariances of the fast and slow shear waves are expressed as:

$$\sigma_{\lambda_1}(0) = \frac{1}{T}\int \lambda_1^2(s)\, ds \quad \text{and} \quad \sigma_{\lambda_2}(0) = \frac{1}{T}\int \lambda_2^2(s)\, ds.$$

The mean values of λ_1 and λ_2 are equal to zero, because the DC component of the data is filtered out.

The maximum of the cross-correlation of the two shear wave time series occurs at time τ. For a noise-free signal, this condition is written:

$$\frac{\partial\rho}{\partial\tau} = \frac{1}{T}\int \lambda_1(t)\dot{\lambda}_2(t+\tau)\, dt = 0.$$

For fast and slow shear waves contaminated by band-limited noise, denoted $n_1(t)$ and $n_2(t)$, the derivative of the two shear wave cross-correlation is

$$\frac{\partial\rho}{\partial\tau} = \frac{1}{T}\int (\lambda_1 + n_1)(t)(\dot{\lambda}_2 + \dot{n}_2)(t+\tau+\delta\tau)\, dt = 0.$$

This derivative vanishes at the time, $\tau+\delta\tau$. Using Taylor expansion of $(\dot{\lambda}_2+\dot{n}_2)(t+\tau+\delta\tau)$ in the noise time series, $n_1(t)$ and $n_2(t)$ and the difference, $\delta\tau$, the perturbation in the time of the maximum of the cross-correlation is up to first order given by:

$$\delta\tau = \frac{-\int \dot{\lambda}_1(t)n_2(t+\tau)\, dt + \int \dot{\lambda}_2(t+\tau)n_1(t)\, dt}{\int \dot{\lambda}_1(t)\dot{\lambda}_2(t+\tau)\, dt}$$

The error in the shear wave time splitting can be estimated as a function of the mean and covariance of the noise time series, $n_1(t)$ and $n_2(t)$:

$$\sigma_\tau^2 = \sum_{ij} \frac{\partial\delta\tau}{\partial n_i}\frac{\partial\delta\tau}{\partial n_j}\sigma_{n_i n_j}^2,$$

The covariance of the time splitting, σ_τ^2, is a function of the covariance and cross-covariance, $\sigma_{n_1}^2$, $\sigma_{n_2}^2$ and $\sigma_{n_1 n_2}^2$, of the noise, associated with the fast and slow shear waves, $n_1(t)$ and $n_2(t)$. Indeed, the fast and slow shear waves and their associated noise are correlated since they are the results of the Alford rotation. In addition, the covariance and cross-covariance of the noise time series after Alford, $n_1(t)$ and $n_2(t)$, are estimated as a function of

the receiver and source misalignment (ϵ_G and ϵ_S), miscoupling (K_G and K_S), and band-limited noise before the Alford rotation (N_{ij}):

$$\sigma_{n_1}^2 = \left(\frac{\partial n_1}{\partial \epsilon_G}\right)^2 \sigma_{\epsilon_G}^2 + \left(\frac{\partial n_1}{\partial \epsilon_S}\right)^2 \sigma_{\epsilon_S}^2 + \left(\frac{\partial n_1}{\partial K_G}\right)^2 \sigma_{K_G}^2$$

$$+ \left(\frac{\partial n_1}{\partial K_S}\right)^2 \sigma_{K_S}^2 + \sum_{ij} \left(\frac{\partial n_1}{\partial N_{ij}}\right)^2 \int \int C_{ij}(t,t')\, dt\, dt'.$$

The receiver misalignment induces an uncertainty in the time splitting as a function of the rotation angle and band-limited noise. For instance, for given noise with a mean of 0.16 and a standard deviation of 0.63, the uncertainty is less than 2 ms, for a misalignment of the receiver of 15° and a S/N of 11 (Figure 4). The uncertainty can exceed 5 ms, for a S/N of 3.5 and reaches 8 ms with a receiver misorientation of 30°.

The S/N ratio is critical in the time splitting estimation. The estimated error in the shear wave time splitting is less than 2 ms, for noise with a S/N noise greater than 10, and attain more than 10 ms, for signal with S/N less than 2 (Figure 5).

The standard deviation in time splitting as a function of the receiver miscoupling and misorientation is less than 2 ms for misorientation less than 15° and a S/N of 11 (Figure 6). The error is larger than 3 ms for 40% of geophone miscoupling. However, for a signal to noise ratio less than 3.5, the uncertainty in polarization angle exceeds 10 ms for a miscoupling of more than 40 % (Figure 7). In this situation, the time splitting of 10 ms cannot be retrieved with statistical significance from these measurements.

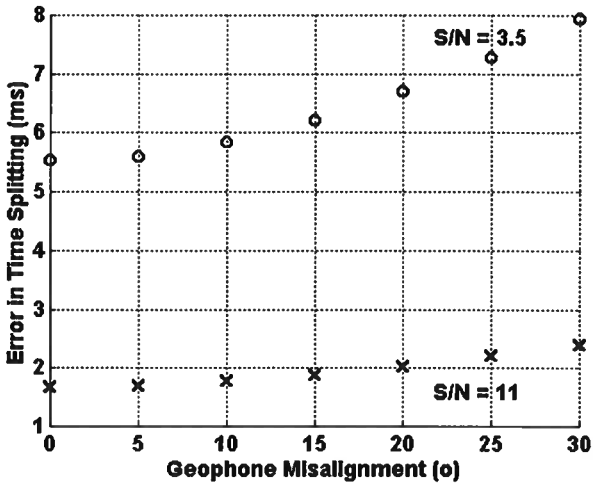

Figure 4. Standard deviation in the shear wave time splitting as a function of the standard deviation of the receiver misalignment and signal to noise ratios. For S/N of 11, the uncertainty is less than 2 ms, for a misalignment of the receiver less than 15°. For S/N of 3.5, the uncertainty is larger than 5 ms, and reaches 8 ms with a receiver misorientation of 30°.

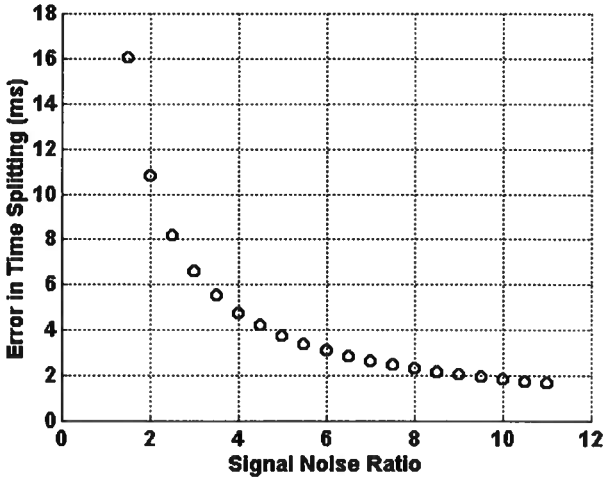

Figure 5. Standard deviation in the shear wave time splitting as a function of the signal to noise ratio. The uncertainty in the time splitting is less than one time sample for a S/N ratio larger than 10.

Conclusions

This analysis has enabled us to derive the uncertainties in shear waves polarization angle and time delay according with error associated to random noise and acquisition uncertainties. This analysis is helpful in interpreting the anisotropy parameters, but also to propose alternative acquisition pattern to record data at a given signal to noise ratio, aimed at minimizing the uncertainty associated with random noise. Another application concerns time-lapse analysis: knowing the uncertainty for each survey, the uncertainty in the change of the seismic attributes can be estimated.

Acknowledgments

The authors are grateful to the members of CWP for helpful discussions. This work has been supported by the Reservoir Characterization Project.

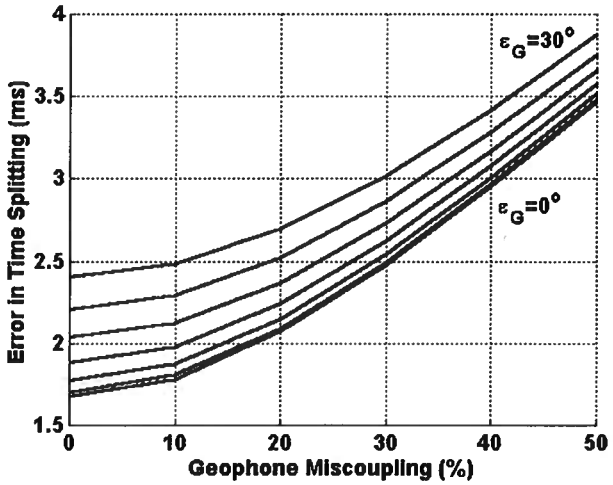

Figure 6. Standard deviation in the shear wave time splitting as a function of receiver miscoupling (σ_{K_G}) and misorientations, for a S/N of 11.

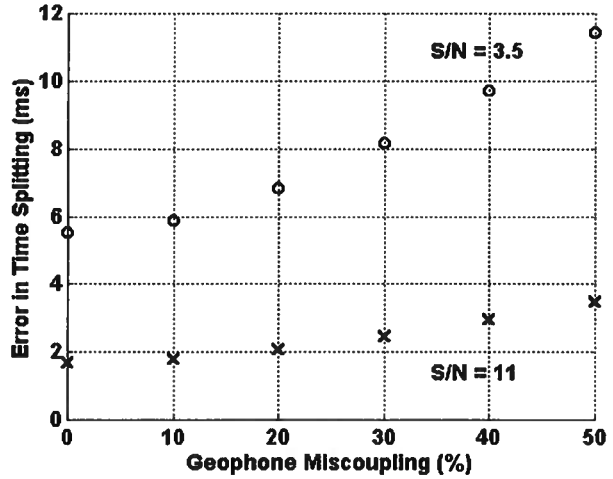

Figure 7. Standard deviation in the shear wave time splitting as a function of receiver miscoupling and signal to noise ratio. For a S/N of 3.5, the uncertainty exceeds 10 ms for a miscoupling of 40%.

References

Alford, R. M., 1986, Shear data in the presence of azimuthal anisotropy: Annual Meeting Abstracts, Society of Exploration Geophysicists, 476-479.

Knowlton, K.B., Spencer, T.W., 1996, Polarization measurement uncertainty on three-component VSP: Geophysics, **61**, 594-599.

Li, X.Y., Crampin, S., 1993, Linear-transform techniques for processing shear- wave anisotropy in four-component seismic data: Geophysics, **58**, 240-256.

MacBeth, C., Zeng, X., Yardley, G., Crampin, S., 1994, Interpreting data matrix asymetry in near-offset, shear-wave VSP data: Geophysics, **59**, 176-191.

Scales, J.A., Snieder, R., 1998, What is noise?: Geophysics, **63**, 1122-1124.

Zeng, X., MacBeth, C., 1993, Algebraic processing techniques for estimating shear-wave splitting in near-offset VSP data: Theory: Geophysical Prospecting, **41**, 1033-1066.